Received: 19 May 2022 | Revised: 31 October 2022 | Accepted: 3 November 2022

DOI: 10.1111/tra.12872

RESEARCH ARTICLE

Traffic WILEY

Multiplexed cellular profiling identifies an organoselenium compound as an inhibitor of CRM1-mediated nuclear export

Lucia Jimenez[1] | Victor Mayoral-Varo[1] | Carlos Amenábar[1,2] | Judit Ortega[1] | João G. N. Sequeira[3] | Miguel Machuqueiro[3] | Cristiana Mourato[4,5] | Romano Silvestri[6] | Andrea Angeli[7] | Fabrizio Carta[7] | Claudiu T. Supuran[7] | Diego Megías[8] | Bibiana I. Ferreira[4,5] | Wolfgang Link[1]

[1]Cancer Biology Department, Instituto de Investigaciones Biomédicas "Alberto Sols" (CSIC-UAM), Madrid, Spain

[2]Departamento de Bioquímica, Universidad Autónoma de Madrid (UAM), Madrid, Spain

[3]BioISI––Instituto de Biosistemas e Ciências Integrativas, Faculdade de Ciências, Universidade de Lisboa, Lisbon, Portugal

[4]ABC-RI, Algarve Biomedical Center Research Institute, Algarve Biomedical Center, Faro, Portugal

[5]Faculty of Medicine and Biomedical Sciences, University of Algarve, Faro, Portugal

[6]Laboratory Affiliated with the Institute Pasteur Italy-Cenci Bolognetti Foundation, Department of Drug Chemistry and Technologies, Sapienza University of Rome, Rome, Italy

[7]Università degli Studi di Firenze, NEUROFARBA Dept., Sezione di Farmaceutica e Nutraceutica, Florence, Italy

[8]Advanced Optical Microscopy Unit, Instituto de salud Carlos III, Madrid, Spain

Correspondence
Wolfgang Link, Instituto de Investigaciones Biomédicas "Alberto Sols" (CSIC-UAM). Arturo Duperier 4. 28029-Madrid, Spain.
Email: walink@iib.uam.es

Bibiana I. Ferreira, ABC-RI, Algarve Biomedical Center Research Institute, Algarve Biomedical Center, Faro, Portugal.
Email: biferreira@ualg.pt

Carlos Amenábar, Departamento de Bioquímica, Universidad Autónoma de Madrid (UAM), Madrid, Spain.
Email: carlos.amenabar@estudiante.uam.es

Funding information
Fundação para a Ciência e a Tecnologia; Spanish Ministry of Science, Innovation and Universities

Abstract

Chromosomal region maintenance 1 (CRM1 also known as Xpo1 and exportin-1) is the receptor for the nuclear export controlling the intracellular localization and function of many cellular and viral proteins that play a crucial role in viral infections and cancer. The inhibition of CRM1 has emerged as a promising therapeutic approach to interfere with the lifecycle of many viruses, for the treatment of cancer, and to overcome therapy resistance. Recently, selinexor has been approved as the first CRM1 inhibitor for the treatment of multiple myeloma, providing proof of concept for this therapeutic option with a new mode of action. However, selinexor is associated with dose-limiting toxicity and hence, the discovery of alternative small molecule leads that could be developed as less toxic anticancer and antiviral therapeutics will have a significant impact in the clinic. Here, we report a CRM1 inhibitor discovery platform. The development of this platform includes reporter cell lines that monitor CRM1 activity by using red fluorescent protein or green fluorescent protein-labeled HIV-1 Rev protein with a strong heterologous nuclear export signal. Simultaneously, the intracellular localization of other proteins, to be interrogated for their capacity to undergo CRM1-mediated export, can be followed by co-culturing stable cell lines expressing fluorescent fusion proteins. We used this platform to interrogate the mode of nuclear export of several proteins, including PDK1, p110α, STAT5A, FOXO1, 3, 4 and TRIB2, and to screen a compound collection. We show that while p110α partially relies on CRM1-dependent nuclear export, TRIB2 is exported from the nucleus in a CRM1-independent manner. Compound screening revealed the striking activity of an organoselenium compound on the CRM1 nuclear export receptor.

KEYWORDS
anticancer drugs, antiviral drugs, biosensors, CRM1, nuclear export, organoselenium compounds, selinexor

1 | INTRODUCTION

The intracellular localization of proteins is often crucial for their functions.[1] Proteins larger than 40 kDa are transported through the nuclear pore complex by soluble nuclear transport receptors such as chromosomal region maintenance 1 (CRM1).[2] CRM1 is expressed in all eukaryotic cells, and an ever-growing number of proteins have been verified as cargoes of CRM1.[3] These proteins generally contain a nuclear export signal (NES) that binds to CRM1.[4] CRM1-mediated nuclear export of viral components is crucial in various stages of the lifecycle and assembly of HIV, human T-cell leukemia virus-1, respiratory syncytial virus, human cytomegalovirus, coronaviruses, influenza, dengue and rabies virus.[5] Accordingly, CRM1 inhibitors have demonstrated activity against over 20 different viruses.[6] The CRM1-assisted export of the HIV-1 Rev protein is crucial for viral RNA transport, and its interruption inhibits the production of new virions and reduces HIV-1 levels.[7] Inhibition of CRM1-mediated export of the influenza viral ribonucleoprotein reduced viral replication, lung viral load and proinflammatory cytokine expression.[8] Similarly, CRM1 is responsible for the nuclear export of several SARS-CoV proteins, including ORF3b,[9,10] ORF9b[11–14] and nucleocapsid N protein,[15,16] and therefore affects SARS-CoV replication and pathogenesis. CRM1 also mediates the nuclear export of a large number of tumor suppressor and oncogenic proteins whose mislocalization drives tumor formation and progression,[17] including p53, FOXO proteins, p27, BCRA1, APC, nucleophosmin and retinoblastoma (Rb), β-catenin, NF-κB, survivin and cyclin D1. Somatic mutations in CRM1 have been identified in human cancer, most of them affecting a single amino acid at position 571.[18] The E571K mutation leads to an increased affinity for NES. The expression of CRM1 is increased in a broad variety of cancer types.[19] High CRM1 expression is correlated with tumor size, metastasis, poor prognosis and drug resistance in many cancer types.[20] Several different CRM1 inhibitors have been shown to sensitize drug-resistant cancer cells to anticancer drugs.[21] Leptomycin B (LMB), a potent antifungal antibiotic from *Streptomyces* sp. was identified as the first CRM1 inhibitor.[22] LMB covalently binds to a cysteine residue at position 528 within the human CRM1 protein and prevents the formation of the cargo-CRM1 complex. Unfortunately, LMB failed in phase I clinical trials because of its high systemic toxicity. The recent clinical approval of selinexor (Xpovio) is proof of concept for the therapeutic utility of manipulating the nuclear export.[23] Despite these encouraging results, selinexor is associated with serious risks, including cytopenias and gastrointestinal toxicity.[24] These side effects limit the dose of selinexor that can be given to patients, which therefore affects the efficacy of the treatment in cancer patients and precludes its development as an antiviral drug. The only known CRM1 inhibitor capable of non-covalent binding to the NES-binding groove is the recently discovered NCI-1.[25] However, in the wild-type form of CRM1, a covalent bond with Cys-528 is still established, resulting in NCI-1 toxicity being similar to other known CRM1 inhibitors. To identify agents capable of inhibiting the CRM1-mediated nuclear export process with less toxicity, screening campaigns using complex collections of diverse small chemical compounds are warranted. There are clear advantages for a screening approach to complement the CRM1 activity analysis with an intracellular localization assessment of other proteins, including known CRM1 substrates, candidate substrates, NES bearing proteins and exported proteins, without an obvious NES or any protein to be analyzed for its capacity to be exported by CRM1. Here, we report the development of a multiplexed CRM1 inhibitor discovery platform that simultaneously monitors the intracellular localization of different reporter proteins. Using this platform, we screened a compound collection of 262 small chemical molecules and identified a selenazole compound as an inhibitor of CRM1-mediated nuclear export, which was also evaluated using molecular docking calculations.

2 | RESULTS

2.1 | Generation and validation of U2redNES reporter cells

We have previously established U2nesRELOC, a screening/counter-screening system that has been successfully used to identify CRM1 inhibitors.[26–29] Based on this reporter system, we developed U2redNES, a stable cell system capable of monitoring CRM1-mediated nuclear export by using the HIV-1 protein Rev[30] with a strong heterologous NES[31] fused to red fluorescent protein (RFP). The generated RFP fusion construct was transfected into osteosarcoma U2OS cells, the genome integration was achieved by antibiotic selection, and resistant cell clones were isolated. Cell clones were amplified, and the distribution of red fluorescence was analyzed in several clones. Cell clones with an exclusive cytoplasmic red fluorescent signal were selected, and the shift of fluorescence into the cell nucleus was confirmed. Since the reporter cell lines will be exposed to chemical compounds dissolved in DMSO, we set out to assess the sensitivity of the generated U2redNES cells to DMSO. U2redNES cells were seeded in 96-well plates and treated with different concentrations of DMSO. Cell toxicity was monitored by visual inspection after 1 h of incubation and cell fixation. This period was chosen as the shift of the fluorescent signal into the cell nucleus is a fast event. As Figure 1 shows, U2redNES displayed no signs of cell toxicity upon exposure to DMSO at concentrations between 0.01% and 0.5% (Figure 1A–E). Nuclear shrinkage and changes in cytoplasmic morphology became visible with DMSO concentrations above 1% (Figure 1F–I). Accordingly, we defined 1% DMSO as the maximum concentration to be used in the U2redNES reporter cells. Next, we determined the kinetics of nuclear accumulation of red reporter protein upon LMB treatment. Cells were seeded at a density of 20 000 cells per well in 96-well plates and exposed to 20 nM LMB for different time points between 10 min and 1 h. LMB failed to affect the subcellular localization of the reporter protein at time points between 10 and 30 min (Figure 1J–M). Red fluorescence started to accumulate in the cell nucleus as a consequence of CRM-1 inhibition after 45 min (Figure 1N). Further nuclear translocation of the fluorescent signal was observed after an incubation period of 1 h (Figure 1O). Based on these results, we decided to carry out all the treatments described in this work for 1 h.

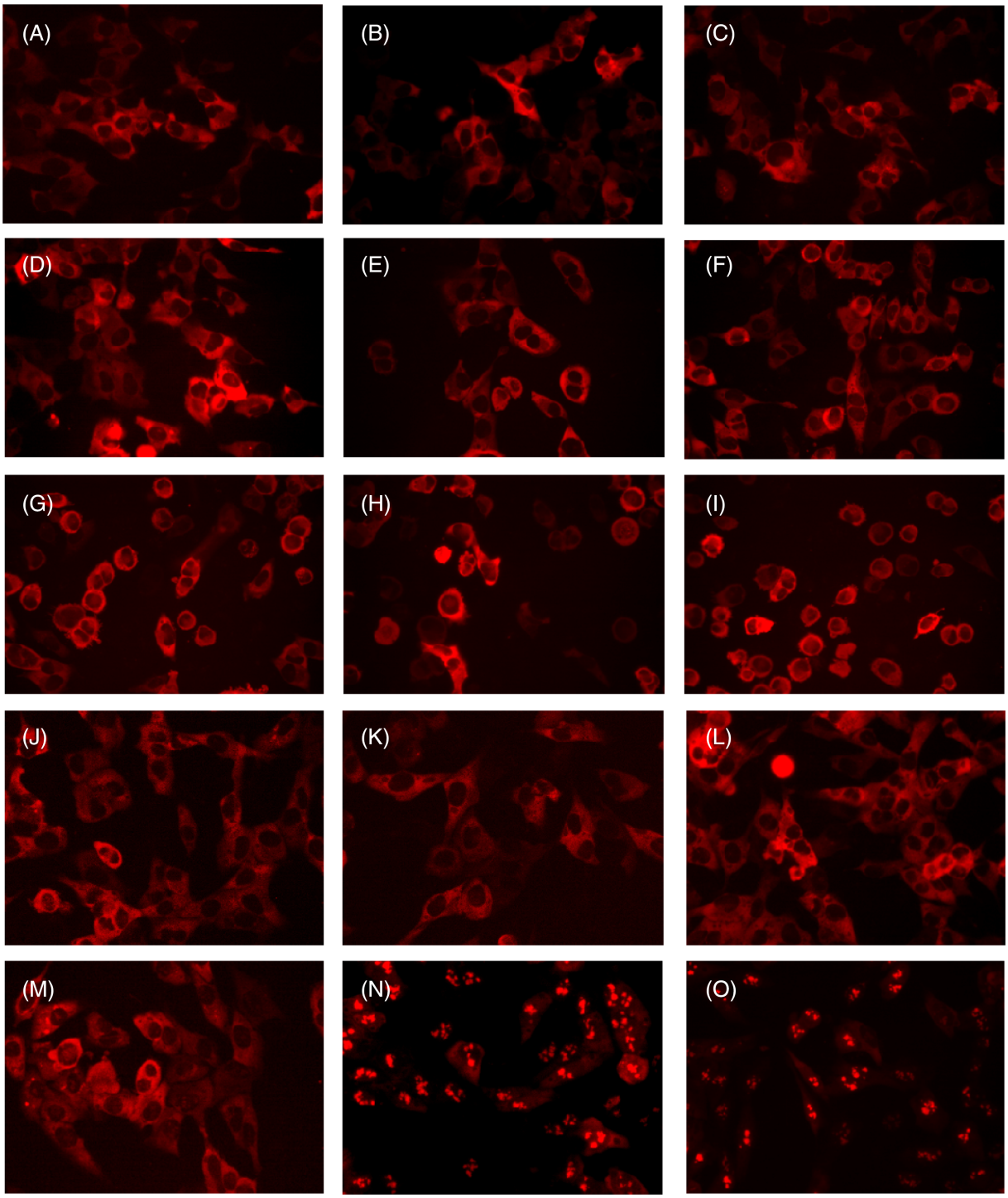

FIGURE 1 Evaluation of reporter cell line sensibility to different DMSO concentrations and time-course of LMB-induced nuclear accumulation of reporter protein. U2redNES cells were (A) untreated or treated with DMSO at (B) 0.01%, (C) 0.05%, (D) 0.1%, (E) 0.5%, (F) 1%, (G) 1.5%, (H) 2% and (I) 2.5%. Kinetics of nuclear accumulation was measured by exposing cells to 20 nM LMB during (J) 0 min, (K) 10 min, (L) 20 min, (M) 30 min, (N) 45 min and (O) 60 min. After 1 h of treatment, cells were fixed with paraformaldehyde, and images were acquired by fluorescent microscopy as detailed in Section 4.

2.2 | Co-culture of U2nesRELOC and U2redNES cells

Multiplexed cellular assays can improve the drug discovery process by simultaneously assessing different molecular events. In order, to determine whether U2nesRELOC and U2redNES can be monitored simultaneously, both cell lines were co-cultured in 96-well plates (10 000 cells of each cell line per well) and treated with LMB concentrations from 0.39 to 100 nM for 1 h. As Figure 2 shows, exposure to LMB at 0.78 nM results in a slight nuclear accumulation of the protein

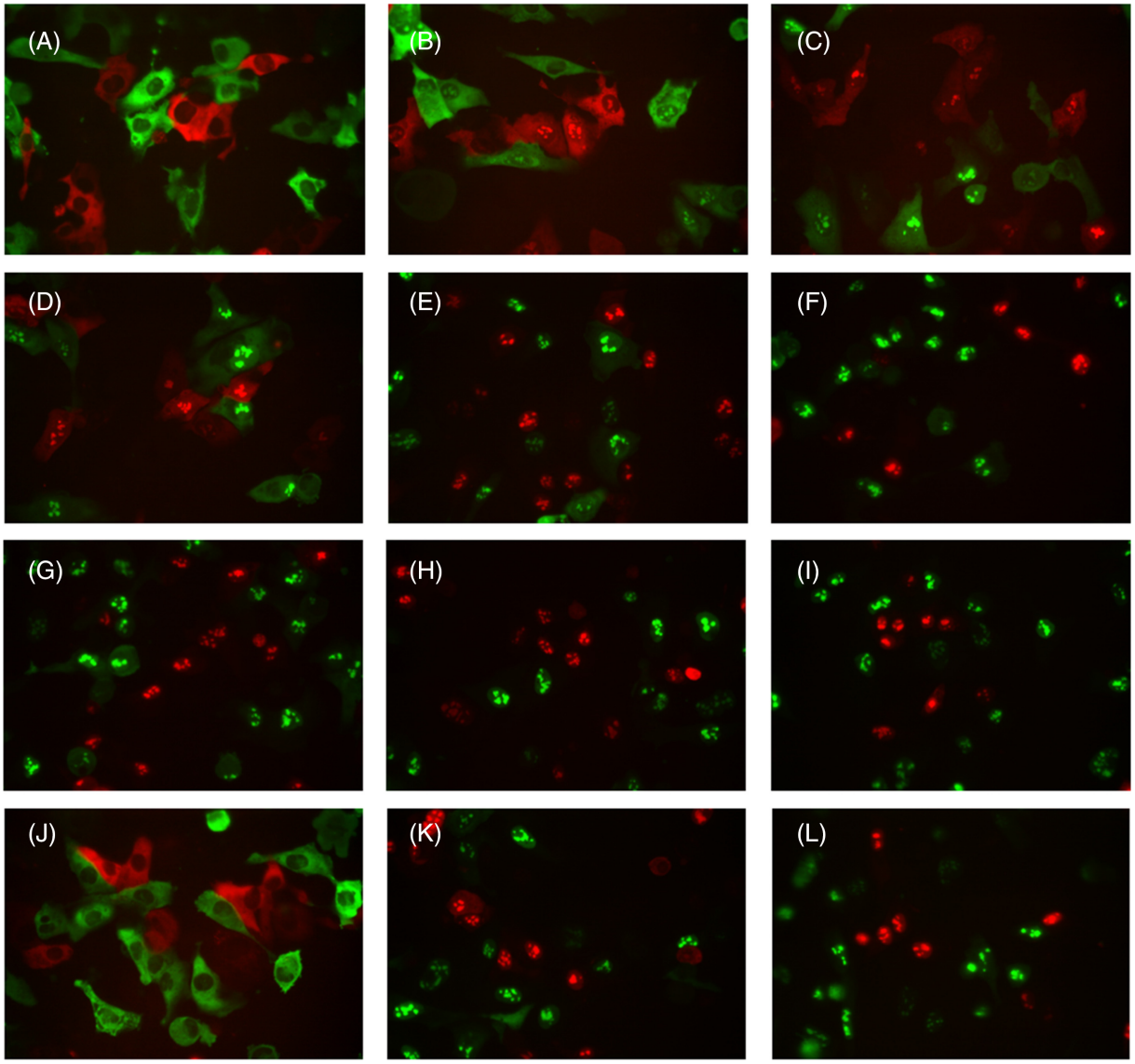

FIGURE 2 Dose–response of LMB and selinexor-induced nuclear translocation of RFP and GFP reporter proteins. U2redNES and U2nesRELOC were co-cultured in 96-well plates and exposed for 1 h to LMB at (A) 0.39 nM, (B) 0.78 nM, (C) 1.56 nM, (D) 3.12 nM, (E) 6.25 nM, (F) 12.5 nM, (G) 25 nM, (H) 50 nM and (I) 100 nM. The clinically approved CRM1 inhibitor selinexor also was tested for 1 h at (J) 10 nM, (K) 50 nM and (L) 100 nM. After compound incubation, cells were fixed, and reporter protein nuclear translocation was quantified by fluorescent microscopy. The ratio of nuclear translocations and (M) EC50 values were calculated compared to control cells treated with DMSO

in both cell lines, which reached its maximum at 25 nM (Figure 2A–I). We use the clinically approved CRM1 inhibitor selinexor to determine whether a different chemical compound with a similar mode of action induced a comparable nuclear translocation of the reporter proteins in both cell lines. After 1 h of exposure to different concentrations of selinexor, the RFP and green fluorescent protein (GFP) fusion proteins shifted to the cell nucleus at 50 and 100 nM (Figure 2J–L). These results indicate that both the red and the green reporter cell lines exhibit similar kinetics and sensitivity to CRM1 inhibition and can be co-cultured to multiplex the assay. Importantly, these features allow us to multiplex the assays with cell lines that express reporter proteins that monitor independent molecular events.

2.3 | Co-culture of U2redNES with green reporter cells

As many as 200 CRM1 substrates have been identified; most of them are proteins that contain a leucine-rich nuclear NES.[4] However, not all NES-containing proteins undergo CRM1-mediated nuclear export, and not all proteins exported by CRM1 possess an obvious NES. As our reporter cell lines can be co-cultured, they have the potential to be multiplexed with other readouts that can monitor the intracellular localization of proteins to be interrogated for their capacity to undergo CRM1-mediated export. To generate compatible assay cell lines, we transfect U2OS and HEK293T cells with different GFP-fusion proteins with known and unexplored

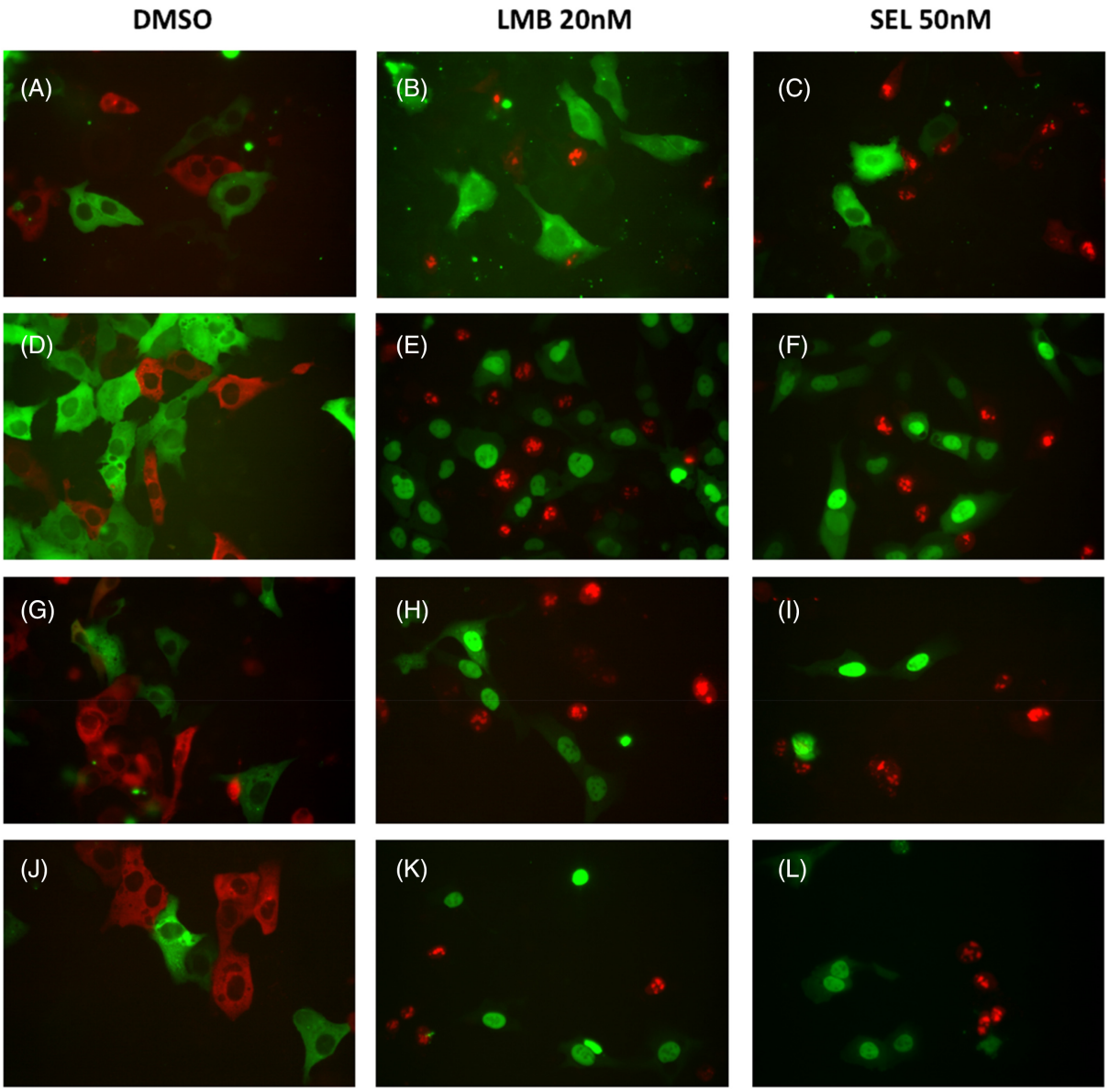

FIGURE 3 Images of multiplexed assay of U2redNES and U2OS transfected with PDK1 and FOXO isoforms fused to GFP and treated with CRM-1 inhibitors. U2redNES were co-cultured with: U2OS cells that expressed PDK1-GFP (A–C), FOXO3a (D–F), FOXO1 (G–I) or FOXO4 (J–L) and were exposed to 1% DMSO (A, D, G and J), 20 nM LMB (B, E, H and K) or 50 nM selinexor (C, F, I and L) for 1 h. After compound exposure, cells were fixed, and images were acquired by fluorescent microscopy.

mechanisms of their nuclear export. The green reporter proteins included 3-phosphoinositide-dependent kinase 1 (PDK1), catalytic p110α subunit of PI3K (p110α), signal transducer and activator of transcription 5A (STAT5A), forkhead box class O transcription factor isoforms FOXO1, 3 and 4 as well as the pseudokinase Tribbles homolog 2 (TRIB2). We co-cultured the resulting green reporter cell lines with U2redNES cells in 96-well plates. Then, cells were exposed to 20 nM LMB, 50 nM selinexor or the vehicle DMSO for 1 h and analyzed by fluorescence microscopy. As Figure 3 shows, these multiplexed assays can be useful to study simultaneously whether a compound of interest acts as a CRM-1 inhibitor, like LMB or selinexor. Furthermore, this multiplexed assay allows for evaluating if the protein fused to GFP is a substrate of CRM1-mediated nuclear export. We observed that known CRM1 substrates, such as PDK1 and the FOXO isoforms FOXO1, FOXO3 and FOXO4, accumulated in the cell nucleus upon CRM1 inhibition with LMB and selinexor in both U2OS and HEK293T cell lines (Figure S1). Conversely, CRM1 inhibition upon LMB and selinexor treatment, monitored by the nuclear accumulation of a red fluorescent signal in U2redNES reporter cells, failed to exert an effect on the subcellular distribution of TRIB2 (Figure 4J–L). This result suggests that the nuclear export of TRIB2 is mediated by a mechanism independent of CRM1. Furthermore, we show that the basal expression of p110α was localized both in the cytoplasm and nucleus of U2OS and HEK293T cells (Figure 4A,D). Treatment with LMB and selinexor enhanced their accumulation in the cell nucleus

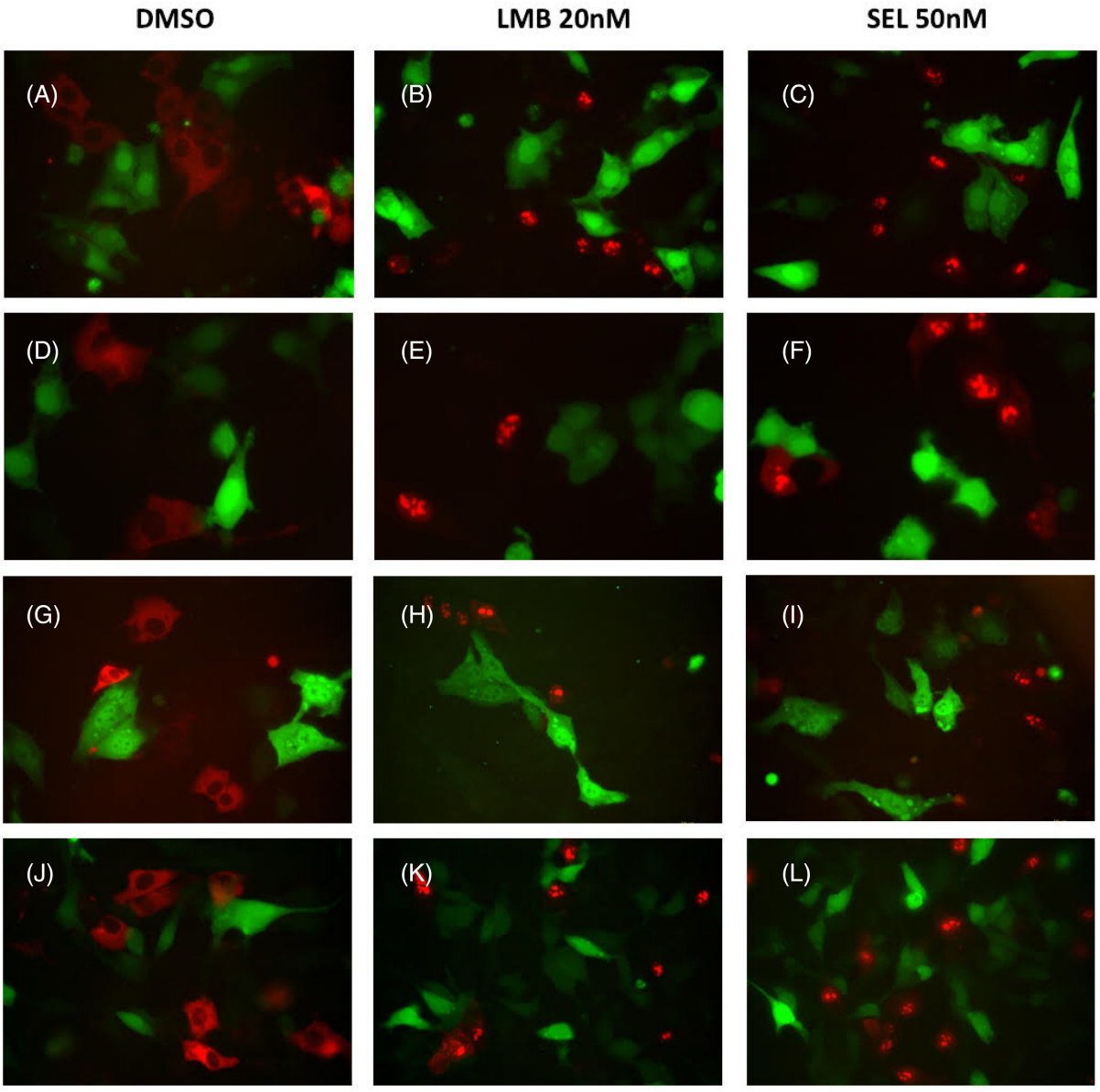

FIGURE 4 Images of the multiplexed assay of U2redNES and U2OS or HEK293T transfected with the catalytic p110α subunit of PI3K, STAT5 and TRIB2 fused to GFP and treated with CRM-1 inhibitors. U2redNES were co-cultured with: U2OS cells that expressed p110α-GFP (A–C), HEK293T transfected with p110α (D–F), STAT5 (G–I) or TRIB2 (J–L) and were exposed to 1% DMSO (A, D, G, and J), 20 nM LMB (B, E, H and K) or 50 nM selinexor (C, F, I and L) for 1 h.

(Figure 4B,C,E,F). In line with other studies,[32] the STAT5A transcription factor is ubiquitously expressed in both cytoplasm and nucleus (Figure 4G), and its nuclear export is mediated by both CRM1-dependent and independent mechanisms since export occurs in the presence of LMB and selinexor (Figure 4H,I).

2.4 | Compound screening

In order to explore if the multiplexed U2redNES is suitable for high-throughput compound screening, we performed a limited screening campaign. We used a collection of 262 small chemical compounds available through several collaborations with chemistry labs all over Europe in the context of several COST actions, namely, CM1407 and CA17104. This COST collection contains compounds with significant structural diversity that have not been previously reported to exert effects on the subcellular localization of FOXO3 or CRM1-mediated nuclear export. The compounds were sent as powders to our lab, dissolved in DMSO as 10 mM stocks, and plated in 96-well compound mother plates at 5 mM. From the compound mother plates, 2 μl of each compound was transferred to the co-cultured U2redNES and U2foxRELOC cells in 96-well assay plates. U2foxRELOC is a previously established reporter cell line based on U2OS cells that stably overexpress FOXO3-GFP.[26,33] The final volume of 200 μl of culture

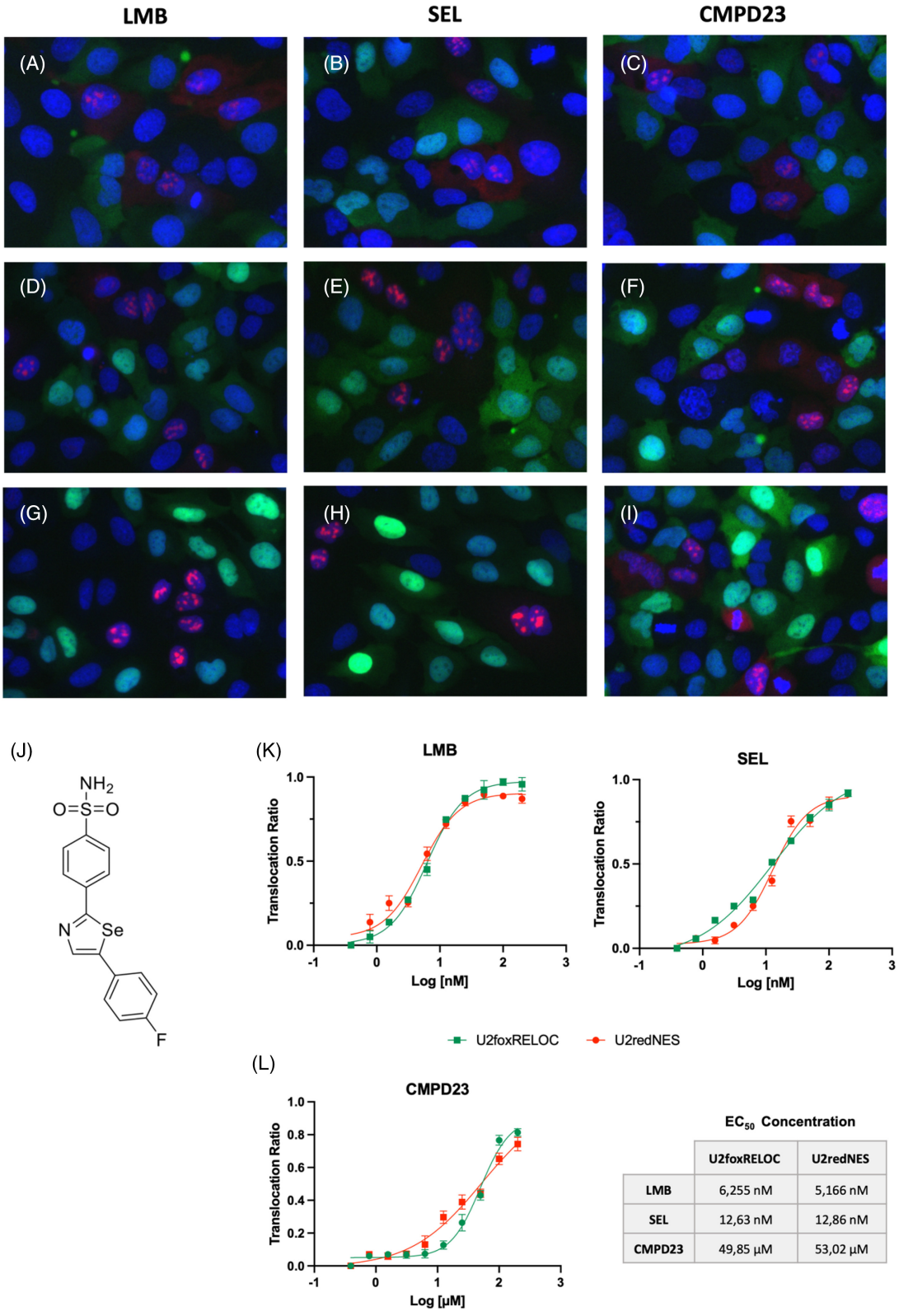

FIGURE 5 The compound screening revealed a selenazole compound with CRM-1 inhibitory activity. U2redNES and U2foxRELOC cells were treated with (A) DMSO, (B) LY294002 at 25 µM, (C) LMB at 20 nM, (D) CMPD23 at 1 µM, (E) CMPD23 at 10 µM, (F) CMPD23 at 25 µM, (G) CMPD23 at 50 µM, (H) CMPD23 at 100 µM and (I) CMPD23 at 200 µM. After incubation time, cells were fixed, and images were acquired by fluorescent microscopy. (J) Chemical structure of CMPD23

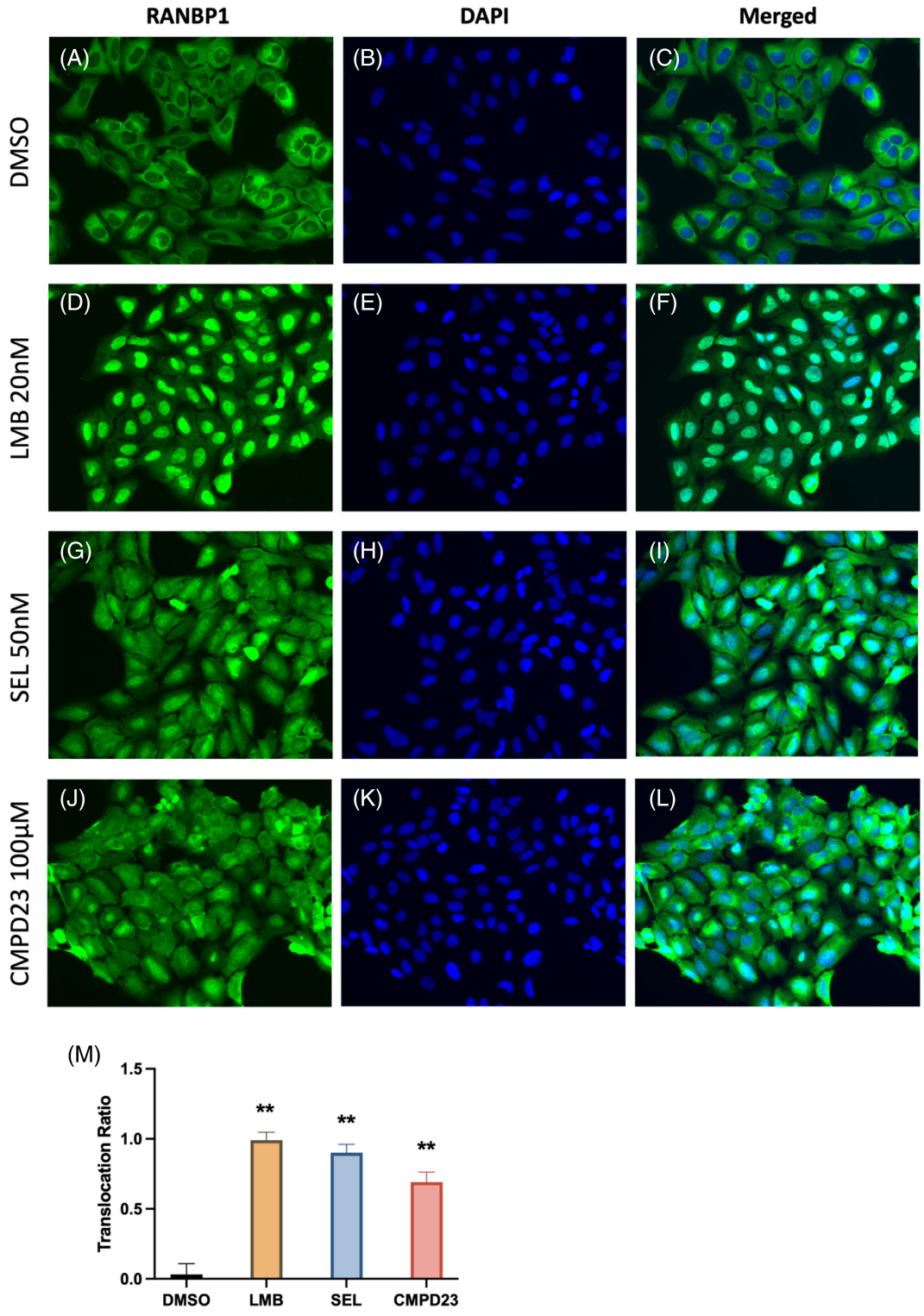

FIGURE 6 Images of U2OS cells treated with vehicle control (DMSO, A–C) 20 nM LMB (D–F), 50 nM selinexor (SEL, G–I) and CMPD23 (J–L). After incubation, cells were fixed, stained and images were acquired by fluorescent microscopy. Cells were stained using a specific antibody against RanBP1 (A, D, G and J), DAPI (B, E, H and K) or merged (C, F, I and L). **, $p < 0.001$.

medium in each well resulted in a final compound concentration of 50 µM. Cells were exposed to the compounds for 1 h, then fixed and the cell nuclei were stained using Hoechst 33342. The primary screening assay revealed the higher activity of the selenazole compound (CMPD23). We performed confirmation screening under identical conditions and validated the activity of the hit compound. We then tested 10 different concentrations of CMPD23 using the procedure described above. Briefly, we co-cultured U2OS with

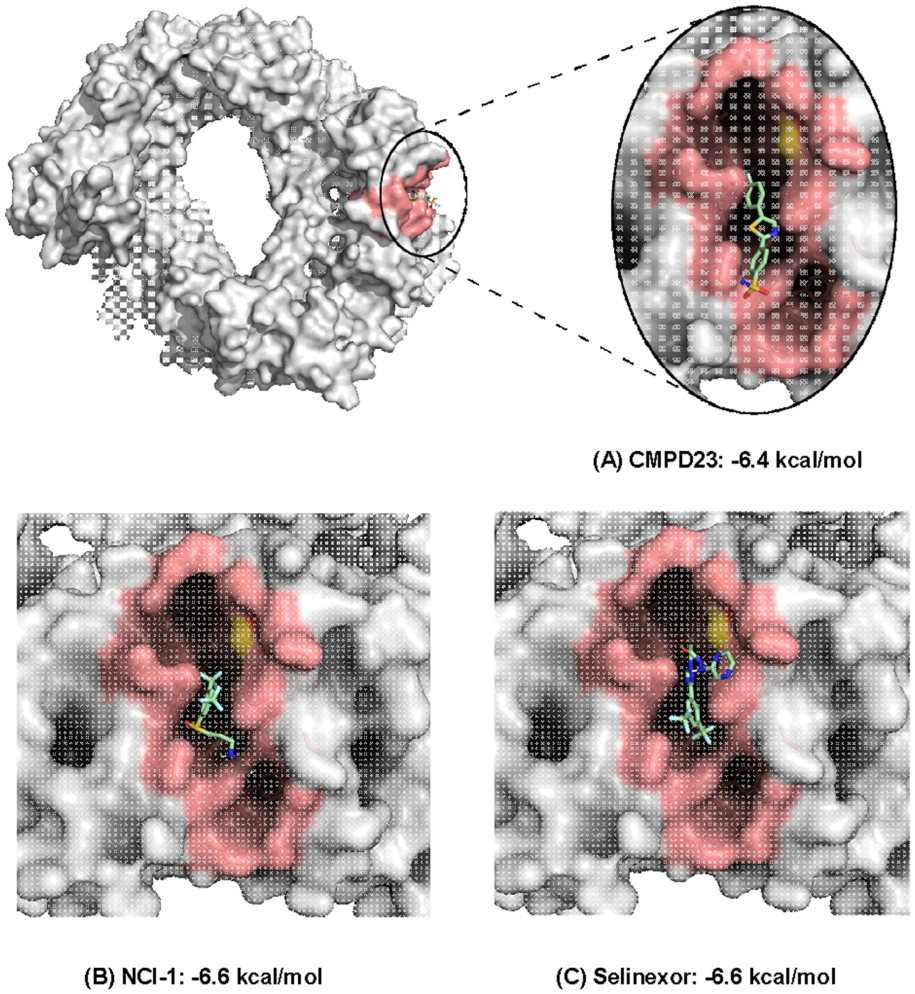

FIGURE 7 CRM1 structure representation and the molecular docking binding modes for CMPD23 (A), NCI-1 (B) and Selinexor (C). CRM1 is represented as a surface colored in white, salmon (NES-binding groove) or yellow (Cys-528). All docked molecules are depicted as sticks with carbon atoms colored in light green

FOXO3-GFP expression and U2redNES in 96-well plates and treated the cells for 1 h with CMPD23, DMSO as a negative control, the PI3K inhibitor LY294002 at 25 μM as a positive control for FOXO3 translocation and LMB and Selinexor also in dose–response as a positive control for CRM-1 inhibition (Figure 5A–I). Dose–response evaluation showed that LMB has a minimal effect in CRM-1 inhibition at 3 nM (Figure 5A) and reaches its maximum at 25 nM (Figure 5G). Selinexor showed an effect at 6 nM (Figure 5B) with a maximum of inhibition at 50 nM (Figure 5E). EC50 values for nuclear accumulation of the red fluorescent signal upon LMB and selinexor treatment of U2redNES cells were 5.166 nM and 12.86 nM, respectively (Figure 5K). CMPD23 exerts its effect on CRM-1 at concentrations of 20 μM and above with an EC50 of 53.02 μM (Figure 5L). CMPD23 as well as LMB and selinexor induced the nuclear translocation of FOXO3 at very similar concentration (49.85 nM, 6.255 nM and 12.69 nM, respectively), suggesting that CMPD23-mediated nuclear accumulation of FOXO3 depends on the inhibition of CRM1 (Figure 5K,L). Figure 5J shows the chemical structure of CMPD23. In order to assess whether CMPD23 also affects other known CRM1 substrates and to confirm that the effect is not limited to ectopically expressed reporter proteins, we used immunocytochemistry to monitor the subcellular localization of endogenous RanBP1 and Cop1. These proteins are well-established CRM1 substrates and have been used to demonstrate the inhibition of CRM1-mediated nuclear export previously.[34,35] As shown in Figure 6, RanBP is exclusively localized in the cytoplasm of untreated U2OS cells. Upon treatment with LMB, endogenous RanBP1 proteins completely shift into the cell nucleus. Exposure to selinexor, but also to CMPD23 induce a significant nuclear accumulation of RanBP1 proteins. Similar results were obtained using a specific antibody against the endogenous Cop1 protein (Figure S2). Molecular docking calculations of CMPD23 in the CRM1 NES-binding groove resulted in a binding mode with a free energy of −6.4 kcal/mol (Figure 7), which is very similar to what was observed for NCI-1 (−6.6 kcal/mol) and selinexor (−6.6 kcal/mol), two known CRM1 inhibitors that bind covalently to Cys-528. Interestingly, other selenazole compounds present in the compound collection failed to exert an effect on CRM1-mediated nuclear export. However, more analogs of CMPD23 need to be evaluated to establish a structure–activity relationship (SAR). A solid SAR could guide medicinal chemistry efforts to optimize CMPD23 and translate our results into useful clinical tools.

3 | DISCUSSION

CRM1 has emerged as a druggable, therapeutic target for the treatment of viral infections and several types of cancer.[20] The current study reports the development of a screening platform to multiplex

the discovery of CRM1 inhibitors with simultaneously monitoring the effect on other related molecular events. We use a stable expression of the HIV-1 protein Rev with a strong heterologous NES fused to either GFP or RFP in the osteosarcoma cell line U2OS. These fluorescent reporter proteins undergo export from the nucleus to the cytoplasm by interacting with the export receptor CRM1 via their NES sequences. Therefore, inhibition of the CRM1 receptor leads to the accumulation of red or green fluorescent signals, which can be detected by a high-content analysis in a high-throughput manner. The design of the assay enables us to multiplex the readout by co-culturing one of these red or green CRM1 reporter cell lines with each other and with other stable cell lines expressing fluorescent fusions of proteins to be interrogated for their capacity to undergo CRM1-mediated nuclear export. To show this capacity of the multiplexed assay, we generated reporter cell lines with proteins known to undergo CRM1-dependent nuclear export like the PDK1[36] and FOXO proteins,[37] as well as proteins known to use several independent mechanisms of nuclear export such as STAT5,[32] and proteins whose mechanism of nuclear export has not been determined such as TRIB2.[38] Our results confirm the CRM1-dependence of PDK1 and FOXO translocation, validating the capacity of our multiplexed reporter assay to provide insights into the molecular mechanisms involved in subcellular protein localization. We observed that STAT5 does not depend on CRM1 for its nuclear export or at least other mechanisms might be able to compensate for the inhibition of CRM1. Conversely, we observed an increased nuclear localization of p110α upon CRM1 inhibition. p110α is the catalytic subunit of the oncogenic lipid kinase PI3Kα, which is the most frequently mutated kinase in human cancer and a major therapeutic target for the development of targeted anticancer drugs.[39] FOXO proteins have been identified as the major transcriptional effectors of PI3K signaling.[40] In agreement with our results, p110α has been reported to exclusively localize in the cell cytoplasm in HEK293 cells.[41] The authors also show a significant nuclear subpopulation of p110α in MCF breast cancer and HCT-116 colon cancer cells. Taken together, these observations and our data suggest that the subcellular localization of p110α is regulated in a cell-specific manner. Importantly, we did not observe any effect of LMB treatment on the subcellular localization of p110α. Interestingly, for the time being, no NES consensus sequences have been identified in the p110α protein. Our data warrant further investigation in assessing the molecular mechanisms of subcellular translocation of this extremely important kinase. In contrast, the subcellular localization of TRIB2 protein present in the cytoplasm, and cell nucleus was not affected by the treatment with LMB or selinexor, which induced a robust nuclear accumulation in the co-cultured CRM1 reporter cells. TRIB2 is a pseudokinase[42] that has been identified as a FOXO repressor protein[43] involved in tumor progression and drug resistance.[44,45] As subcellular localization is the major mechanism to regulate the activity of FOXO transcription factors, understanding the mechanisms underlying the subcellular translocation of the FOXO repressor TRIB2 is of critical interest. Our data suggest that the nuclear export of TRIB2 is CRM1-independent. Accordingly, TRIB2 lacks a NES consensus sequence, and the nuclear export receptor responsible for the TRIB2 nuclear export remains to be identified. As ectopic expression can potentially affect the subcellular localization of proteins, we used immunocytochemistry to show that FOXO3 does not behave differently upon LMB treatment depending on whether it is expressed endogenously or ectopically. Our study also suggests that the experimental design allows for the multiplexed interrogation of any protein of choice, enabling systematic studies of proteins whose nuclear export mechanism is unknown. Multiplexing of green U2nesRELOC and red U2redNES cells could also be used to assess CRM1 function by genetic interrogation in one cell line and using the other cell lines as a control in the same experiment or well. Importantly, we showed that our multiplexed assay system is suitable for large-scale analysis of chemical compounds. Out of a collection of 262 small compounds, we identified the selenazole compound CMPD23 as a CRM1 inhibitor capable of trapping the NES-bearing tumor suppressor protein FOXO3 into the cell nucleus. The relatively modest docking binding energy of CMPD23 in the NES-binding groove of the CRM1 crystal structure indicates that it may bind significantly different from leptomycin B (it was bound to Cys528 in the original crystal structure) or its inhibitory activity may be exerted in a different CRM1 pocket. Therefore, further in silico studies exploring different NES-binding groove conformations are required to fully evaluate the potential of CMPD23 as a non-covalent CRM1 inhibitor. Organoselenium compounds have been extensively studied for their pharmacological properties as antitumor, antiviral, antimicrobial and antihypertensive agents, as well as antioxidants.[46] Inhibitory action of these compounds has been reported for several enzymes, including carbonic anhydrase,[47] nitric oxide synthase[48] and lipoxygenase.[49] The current study is the first, to the best of our knowledge, to reveal a striking activity of an organoselenium compound on the CRM1 nuclear export receptor. Further investigations will elucidate whether this is a common feature of this compound class and what is the real contribution of CMPD23 CRM1 inhibition activity to its antitumor and antiviral properties.

4 | MATERIALS AND METHODS

4.1 | Compounds

Selinexor and LY294002 were purchased from Selleck Chemicals. CMPD23 was part of a collection of 262 small chemical compounds available through several collaborations with chemistry labs all over Europe in the context of several COST actions, namely, CM1407 and CA17104. Leptomycin B was purchased from Alamone labs. CMPD23 was obtained as reported previously.[50]

4.2 | Plasmids

To generate the red fluorescent reporter cell line, we based it on the reporter cell line U2nesRELOC that expresses the construct pRev$_{MAPKK}$GFP, which has been described earlier.[26–29] pRev$_{MAPK-K}$nesGFP carries the NES from MAPK kinase (MAPKK) cloned in

pRev(1.4)-GFP, sandwiched between the Rev and the GFP coding sequences. We exchanged the GFP protein for monomeric RFP by cloning the mRFP from a pmRFP-N1 between AgeI and NotI restriction sites, obtaining the $pRev_{MAPKK}RFP$ construct.

4.3 | Cell culture and stable transfections

The stable reporter cell lines U2foxRELOC[27,29] and U2nesRELOC[26–29] were generated previously. These cell lines, as well as U2OS parental cells and HEK293T2 cells, were maintained in DMEM supplemented with 10% FBS (Sigma) and antibiotics (Gibco). Cell cultures were maintained in a humified incubator at 37°C with 5% CO_2 and passaged when confluent using trypsin/EDTA. Transfection of $pRev_{MAPKK}RFP$ was performed using Lipofectamine 2000 transfection reagent (Invitrogen) according to the manufacturer's instructions. Forty-eight hours after transfection, cells were selected with 800 μl/ml G418 for 10 days. After antibiotic selection, cell clones with an exclusive cytoplasmic red fluorescent signal were isolated, and the shift of fluorescent signals into the cell nucleus was confirmed by using LMB 20 nM.

4.4 | Co-culture of cell lines

U2OS and HEK293T were transiently transfected with reporter plasmids expressing PDK1, p110α, STAT5, TRIB2 or FOXO isoforms using Lipofectamine 2000 (Invitrogen) according to the manufacturer's instructions. Forty-eight hours after transfection, GFP expression was confirmed by fluorescent microscopy. U2redNES and transiently transfected U2OS/HEK cells were seeded at a density of 10^4 cells/well for each cell type into black, clear-bottom 96-well microplates (BD Biosciences). After 24 h of incubation, 2 μl of each compound (100× concentrated) were added in quadruplicated, and cells were incubated for 1 h (except for the time course assay, where cells were incubated from 10 min to 1 h). Then cells were fixed with 4% paraformaldehyde. Finally, the plates were washed with 1× phosphate-buffered saline and stored at 4°C before analysis.

4.5 | Image analysis and EC50 calculation

Cells images were taken in DMIL LED FLUO inverted microscope (Leica) at 40-fold magnification.

The effective concentration (EC50) value of LMB represents the concentration of LMB that exerts 50% of its maximal response. It was determined by regression analysis, using a Quest Graph™ EC50 Calculator (www.aatbio.com). For fluorescent translocation analysis, images were acquired with a Leica Thunder Imager (DMI-8, Leica Microsystems) using a 20× PLAPO 0.8 NA dry objective. Images were analyzed by using Cell Profiler,[51] analysis pipeline identified the nucleus in the blue channel (DNA), and cytoplasms using green or red fluorescent channels, the ratio between the nucleus and cytoplasm was calculated. The translocation cell phenotype percentage is calculated first by discarding possible negative cells and then by setting up two thresholds (one for green cells and another for red positive cells).

4.6 | Molecular docking

All molecular docking calculations were performed with AutoDock 4,[52] which has a detailed scoring function with a high correlation to experimental binding affinities.[53] We used the human CRM1 crystal structure (PDB ID: 6TVO[54]), which was cocrystallized with a bound leptomycin B molecule, which was stripped. The CMPD23, selinexor and NCI-1 structures were optimized (energy-minimized) using Gaussian 09,[55] at the B3LYP[56–58] level of theory and the 6-31G* basis set. The NCI-1 compound is a Lewis base; hence, the adopted protonated secondary amine should be the most representative state at physiological pH. AutoDock Tools[2] was used to set the torsion in all ligands, resulting in four rotatable bonds for CMPD23, five for selinexor and nine for NCI-1.

All interactions between ligand and receptor were explored by the AutoDock Lamarckian Genetic (LGA) algorithm. The hydrogen bonding and Van der Waals terms were calculated using AutoDock default parameters, while the electrostatic interactions were computed using the dielectric function of Mehler and Solmajer.[59] A total of 1000 LGA runs (docking solutions) were performed for each ligand using standard AutoDock parameters except for the number of individuals in the population (300) and the maximum number of energy evaluations (3.5×10^7). In the clustering procedure, an RMS tolerance of 1.5 Å was adopted for all ligands.

AUTHOR CONTRIBUTIONS

Lucia Jimenez designed and performed experiments, analyzed data and wrote the manuscript; Victor Mayoral-Varo, Carlos Amenábar, Cristiana Mourato and Judit Ortega carried out experiments. Diego Megías performed experiments and image analysis, and João G.N. Sequeira performed the molecular docking calculations. Miguel Machuqueiro discussed the results and provided computational chemistry expertise; Romano Silvestri, Fabrizio Carta and Claudiu T. Supuran provided chemical compounds; Andrea Angeli synthesized CMPD23; and Bibiana I.Ferreira designed experiments. Wolfgang Link designed and supervised the research and drafted the manuscript. All authors contributed to the completion of the manuscript.

ACKNOWLEDGMENTS

This article is based upon work from COST Action STRATAGEM, CA17104, supported by COST (European Cooperation in Science and Technology) (www.cost.eu, accessed in March 2022). Romano Silvestri is indebted to AIRC, IG 2020, code no. 24703. This work was supported by the Spanish Ministry of Science, Innovation and Universities through Grant RTI2018-094629-B-I00 to Wolfgang Link. Miguel Machuqueiro thanks Fundação para a Ciência e Tecnologia (Portugal) for CEECIND/02300/2017 (grant), UIDB/04046/2020 and UIDP/04046/2020 (projects).

CONFLICT OF INTEREST

The authors declare no conflict of interest. Wolfgang Link is the scientific co-founder of Refoxy Pharmaceuticals GmbH, Berlin, and is required by his institution to state so in his publications. The funders had no role in the design and writing of the manuscript.

PEER REVIEW

The peer review history for this article is available at https://publons.com/publon/10.1111/tra.12872.

DATA AVAILABILITY STATEMENT

Additional supporting information may be found in the online version of the article at the publisher's website.

ORCID

João G. N. Sequeira https://orcid.org/0000-0003-3246-5964
Miguel Machuqueiro https://orcid.org/0000-0001-6923-8744
Cristiana Mourato https://orcid.org/0000-0003-1402-9747
Bibiana I. Ferreira https://orcid.org/0000-0003-4772-9395
Wolfgang Link https://orcid.org/0000-0002-3340-5165

REFERENCES

1. Hung MC, Link W. Protein localization in disease and therapy. *J Cell Sci*. 2011;124:3381-3392. http://www.ncbi.nlm.nih.gov/pubmed/22010196
2. Wing CE, HYJ F, Chook YM. Karyopherin-mediated nucleocytoplasmic transport. *Nat Rev Mol Cell Biol*. 2022;23:307-328. https://www.nature.com/articles/s41580-021-00446-7
3. Sun Q, Chen X, Zhou Q, Burstein E, Yang S, Jia D. Inhibiting cancer cell hallmark features through nuclear export inhibition. *Signal Transduct Target Ther*. 2016;1:16010.
4. Lee Y, Baumhardt JM, Pei J, Chook YM, Grishin NV. pCRM1exportome: database of predicted CRM1-dependent nuclear export signal (NES) motifs in cancer-related genes. *Bioinformatics*. 2020;36:961-963. https://academic.oup.com/bioinformatics/article/36/3/961/5553090
5. Mathew C, Ghildyal R. CRM1 inhibitors for antiviral therapy. *Front Microbiol*. 2017;8:1171.
6. Kashyap T, Murray J, Walker CJ, et al. Selinexor, a novel selective inhibitor of nuclear export, reduces SARS-CoV-2 infection and protects the respiratory system in vivo. *Antiviral Res*. 2021;192:105115.
7. Najera I, Krieg M, Karn J. Synergistic stimulation of HIV-1 Rev-dependent export of unspliced mRNA to the cytoplasm by hnRNP A1. *J Mol Biol*. 1999;285:1951-1964.
8. Perwitasari O, Johnson S, Yan X, et al. Verdinexor, a novel selective inhibitor of nuclear export, reduces influenza a virus replication In vitro and In vivo. *J Virol*. 2014;88:10228-10243.
9. Konno Y, Kimura I, Uriu K, et al. SARS-CoV-2 ORF3b is a potent interferon antagonist whose activity is increased by a naturally occurring elongation variant. *Cell Rep*. 2020;32:108185.
10. Freundt EC, Yu L, Park E, Lenardo MJ, Xu X-N. Molecular determinants for subcellular localization of the severe acute respiratory syndrome coronavirus open Reading frame 3b protein. *J Virol*. 2009;83:6631-6640.
11. Jiang H wei, Zhang H nan, Meng Q feng, Xie J, Li Y, Chen H, Zheng Y xiao, Wang X ning, Qi H, Zhang J, Wang PH, Han ZG, Tao SC. SARS-CoV-2 Orf9b suppresses type I interferon responses by targeting TOM70. *Cell Mol Immunol* 2020 17:998–1000. https://www.nature.com/articles/s41423-020-0514-8
12. Moshynskyy I, Viswanathan S, Vasilenko N, et al. Intracellular localization of the SARS coronavirus protein 9b: evidence of active export from the nucleus. *Virus Res*. 2007;127:116 Available from: /pmc/articles/PMC7114319/.
13. Sharma K, Åkerström S, Sharma AK, et al. SARS-CoV 9b protein diffuses into nucleus, undergoes active Crm1 mediated nucleocytoplasmic export and triggers apoptosis when retained in the nucleus. *PLoS One*. 2011;6:e19436. doi:10.1371/journal.pone.0019436
14. Shi C-S, Qi H-Y, Boularan C, et al. SARS-coronavirus open Reading frame-9b suppresses innate immunity by targeting mitochondria and the MAVS/TRAF3/TRAF6 signalosome. *J Immunol*. 2014;193:3080-3089. https://www.jimmunol.org/content/193/6/3080
15. Li JY, Liao CH, Wang Q, et al. The ORF6, ORF8 and nucleocapsid proteins of SARS-CoV-2 inhibit type I interferon signaling pathway. *Virus Res*. 2020;286:198074.
16. You JH, Reed ML, Hiscox JA. Trafficking motifs in the SARS-coronavirus nucleocapsid protein. *Biochem Biophys Res Commun*. 2007;358:1015 Available from: /pmc/articles/PMC7092899/.
17. Hill R, Cautain B, De Pedro N, Link W. Targeting nucleocytoplasmic transport in cancer therapy. *Oncotarget*. 2014;5(1):11-28.
18. Puente XS, Pinyol M, Quesada V, et al. Whole-genome sequencing identifies recurrent mutations in chronic lymphocytic leukaemia. *Nature*. 2011;475:101-105.
19. Ferreira BI, Cautain B, Grenho I, Link W. Small molecule inhibitors of CRM1. *Front Pharmacol*. 2020;11:625.
20. Azmi AS, Uddin MH, Mohammad RM. The nuclear export protein XPO1—from biology to targeted therapy. *Nat Rev Clin Oncol*. 2020;18:152-169. https://www.nature.com/articles/s41571-020-00442-4
21. Turner JG, Dawson J, Sullivan DM. Nuclear export of proteins and drug resistance in cancer. *Biochem Pharmacol*. 2012;83:1021-1032.
22. Kudo N, Wolff B, Sekimoto T, et al. Leptomycin B inhibition of signal-mediated nuclear export by direct binding to CRM1. *Exp Cell Res*. 1998;242:540-547. https://linkinghub.elsevier.com/retrieve/pii/S0014482798941362
23. Chari A, Vogl DT, Gavriatopoulou M, et al. Oral Selinexor––dexamethasone for triple-class refractory multiple myeloma. *N Engl J Med*. 2019;381:727-738.
24. Hashmi H, Green K. The 'comeback' of selinexor: from toxic to tolerable. *Curr Probl Cancer*. 2022;46(1):100789.
25. Lei Y, An Q, Shen XF, et al. Structure-guided design of the first non-covalent small-molecule inhibitor of CRM1. *J Med Chem*. 2021;64:6596-6607. doi:10.1021/acs.jmedchem.0c01675
26. Zanella F, Rosado A, Blanco F, Henderson BR, Carnero A, Link W. An HTS approach to screen for antagonists of the nuclear export machinery using high content cell-based assays. *Assay Drug Dev Technol*. 2007;5:333-341. http://www.ncbi.nlm.nih.gov/pubmed/17638533
27. Link W, Oyarzabal J, Serelde BG, et al. Chemical interrogation of FOXO3a nuclear translocation identifies potent and selective inhibitors of phosphoinositide 3-kinases. *J Biol Chem*. 2009;284:28392-28400. http://www.ncbi.nlm.nih.gov/pubmed/19690175
28. Cautain B, de Pedro N, Murillo Garzon V, et al. High-content screening of natural products reveals novel nuclear export inhibitors. *J Biomol Screen*. 2014;19:57-65. http://www.ncbi.nlm.nih.gov/pubmed/24045581
29. Jimenez L, Silva A, Calissi G, et al. Screening health-promoting compounds for their capacity to induce the activity of FOXO3. *Journals Gerontol Ser A*. 2022;77(8):1485-1493. doi:10.1093/gerona/glab265/6368778
30. Pollard VW, Malim MH. The HIV-1 Rev protein. *Annu Rev Microbiol*. 1998;52:491-532. doi:10.1146/annurev.micro.52.1.491
31. Henderson BR, Eleftheriou A. A comparison of the activity, sequence specificity, and CRM1-dependence of different nuclear export signals. *Exp Cell Res*. 2000;256:213-224.
32. Shin HY, Reich NC. Dynamic trafficking of STAT5 depends on an unconventional nuclear localization signal. *J Cell Sci*. 2013;126:3333-3343. https://journals.biologists.com/jcs/article/126/15/3333/53762/Dynamic-trafficking-of-STAT5-depends-on-an

33. Zanella F, Rosado A, Garcia B, Carnero A, Link W. Chemical genetic analysis of FOXO nuclear-cytoplasmic shuttling by using image-based cell screening. *Chembiochem*. 2008;9:2229-2237. http://www.ncbi.nlm.nih.gov/pubmed/18756565
34. Plafker K, Macara IG. Facilitated nucleocytoplasmic shuttling of the ran binding protein RanBP1. *Mol Cell Biol*. 2000;20:3510-3521. doi:10.1128/MCB.20.10.3510-3521.2000
35. Choi HH, Guma S, Fang L, et al. Regulating the stability and localization of CDK inhibitor p27Kip1 via CSN6-COP1 axis. 2015;14:2265-2273. doi:10.1080/15384101.2015.1046655
36. Scheid MP, Parsons M, Woodgett JR. Phosphoinositide-dependent phosphorylation of PDK1 regulates nuclear translocation. *Mol Cell Biol* [Internet] 2005;25:2347–2363. 10.1128/MCB.25.6.2347-2363.2005
37. Calissi G, Lam EWF, Link W. Therapeutic strategies targeting FOXO transcription factors. *Nat Rev Drug Discov*. 2021;20:21-38. https://www.nature.com/articles/s41573-020-0088-2
38. Mayoral-Varo V, Jiménez L, Link W. The critical role of TRIB2 in cancer and therapy resistance. *Cancers (Basel)*. 2021;13:2701. https://www.mdpi.com/2072-6694/13/11/2701
39. Wong KK, Engelman JA, Cantley LC. Targeting the PI3K signaling pathway in cancer. *Curr Opin Genet Dev*. 2010;20:87-90.
40. Hill R, RKR K, Callejas S, et al. A novel phosphatidylinositol 3-kinase (PI3K) inhibitor directs a potent FOXO-dependent, p53-independent cell cycle arrest phenotype characterized by the differential induction of a subset of FOXO-regulated genes. *Breast Cancer Res*. 2014;16:482 http://www.ncbi.nlm.nih.gov/pubmed/25488803
41. Singh P, Dar MS, Singh G, et al. Dynamics of GFP-fusion p110α and p110β isoforms of PI3K signaling pathway in Normal and cancer cells. *J Cell Biochem*. 2016;117:2864-2874. doi:10.1002/jcb.25598
42. Eyers PA, Keeshan K, Kannan N. Tribbles in the 21st century: the evolving roles of tribbles pseudokinases in biology and disease. *Trends Cell Biol*. 2017;27:284-298. https://linkinghub.elsevier.com/retrieve/pii/S0962892416301787
43. Zanella F, Renner O, Garcia B, et al. Human TRIB2 is a repressor of FOXO that contributes to the malignant phenotype of melanoma cells. *Oncogene*. 2010;29:2973-2982. http://www.ncbi.nlm.nih.gov/pubmed/20208562
44. Hill R, Kalathur RK, Colaco L, et al. TRIB2 as a biomarker for diagnosis and progression of melanoma. *Carcinogenesis*. 2015;36:469-477. http://www.ncbi.nlm.nih.gov/pubmed/25586991
45. Hill R, Madureira PA, Ferreira B, et al. TRIB2 confers resistance to anti-cancer therapy by activating the serine/threonine protein kinase AKT. *Nat Commun*. 2017;8:1-9.
46. Nogueira CW, Zeni G, JBT R. Organoselenium and organotellurium compounds: toxicology and pharmacology. *Chem Rev*. 2004;104:6255-6285. doi:10.1021/cr0406559
47. Angeli A, Tanini D, Viglianisi C, et al. Evaluation of selenide, diselenide and selenoheterocycle derivatives as carbonic anhydrase I, II, IV, VII and IX inhibitors. *Bioorg Med Chem*. 2017;25:2518-2523.
48. Wang J-F, Komarov P, Sies H, de Groot H. Inhibition of superoxide and nitric oxide release and protection from reoxygenation injury by ebselen in rat kupffer cells. *Hepatology*. 1992;15:1112-1116. doi:10.1002/hep.1840150623
49. Schewe C, Schewe T, Wendel A. Strong inhibition of mammalian lipoxygenases by the antiinflammatory seleno-organic compound ebselen in the absence of glutathione. *Biochem Pharmacol*. 1994;48:65-74.
50. Angeli A, Trallori E, Ferraroni M, Di Cesare ML, Ghelardini C, Supuran CT. Discovery of new 2, 5-disubstituted 1,3-selenazoles as selective human carbonic anhydrase IX inhibitors with potent antitumor activity. *Eur J Med Chem*. 2018;157:1214-1222.
51. Carpenter AE, Jones TR, Lamprecht MR, et al. CellProfiler: image analysis software for identifying and quantifying cell phenotypes. *Genome Biol*. 2006;7:1-11. doi:10.1186/gb-2006-7-10-r100
52. Morris GM, Ruth H, Lindstrom W, et al. AutoDock4 and AutoDockTools4: automated docking with selective receptor flexibility. *J Comput Chem*. 2009;30:2785-2791. doi:10.1002/jcc.21256
53. Nguyen NT, Nguyen TH, TNH P, et al. Autodock Vina adopts more accurate binding poses but Autodock4 forms better binding affinity. *J Chem Inf Model*. 2020;60:204-211. doi:10.1021/acs.jcim.9b00778
54. Shaikhqasem A, Dickmanns A, Neumann P, Ficner R. Characterization of inhibition reveals distinctive properties for human and saccharomyces cerevisiae CRM1. *J Med Chem*. 2020;63:7545-7558. doi:10.1021/acs.jmedchem.0c00143
55. G09. 2022; https://gaussian.com/glossary/g09/
56. Becke AD. Density-functional exchange-energy approximation with correct asymptotic behavior. *Phys Rev A*. 1988;38:3098-3100. doi:10.1103/PhysRevA.38.3098
57. Lee C, Yang W, Parr RG. Development of the Colle-Salvetti correlation-energy formula into a functional of the electron density. *Phys Rev B*. 1988;37:785. doi:10.1103/PhysRevB.37.785
58. Vosko SH, Wilk L, Nusair M. Accurate spin-dependent electron liquid correlation energies for local spin density calculations: a critical analysis. *Canadian Journal of Physics*. 1980;58:1200-1211. doi:10.1139/p80-159
59. Mehler EL, Solmajer T. Electrostatic effects in proteins: comparison of dielectric and charge models. *Protein Eng Des Sel*. 1991;4:903-910. https://academic.oup.com/peds/article/4/8/903/1439191

SUPPORTING INFORMATION

Additional supporting information can be found online in the Supporting Information section at the end of this article.

How to cite this article: Jimenez L, Mayoral-Varo V, Amenábar C, et al. Multiplexed cellular profiling identifies an organoselenium compound as an inhibitor of CRM1-mediated nuclear export. *Traffic*. 2022;23(12):587-599. doi:10.1111/tra.12872